

PRECISION MEASUREMENT OF THE HIGGS BOSON MASS AND SEARCH FOR
DILEPTON MASS RESONANCES IN $H \rightarrow 4\ell$ DECAYS USING THE CMS DETECTOR AT
THE LHC

By

JAKE ROSENZWEIG

A DISSERTATION PRESENTED TO THE GRADUATE SCHOOL
OF THE UNIVERSITY OF FLORIDA IN PARTIAL FULFILLMENT
OF THE REQUIREMENTS FOR THE DEGREE OF
DOCTOR OF PHILOSOPHY

UNIVERSITY OF FLORIDA

2022

© 2022 Jake Rosenzweig

This work is dedicated to the living and loving memory of Jacob Myhre.

ACKNOWLEDGEMENTS

Without so many two- and four-legged blessings along the way, I could never have made it to this point in my academic career. Thus, I begin by giving my endless gratitude to my high energy physics mentors, Professors Andrey Korytov and Guenkah Mitselmakher, for granting me this one-of-a-kind opportunity to do real *science* at CERN.

To my wife, Suzanne Rosenzweig, for showing me that dreams *do* come true. To my mother and father, Vicki and John, who always reassured me that I could achieve anything I put my mind to. Sleep peacefully, Mom. To my siblings, Alex, Ryan, Devin, Jace, and Claudia who frequently and gently reminded me that life existed outside of grad school. To Auntie Rachel and Uncle Yuri, who just *get* me and have given to me everything I could have possible asked for. To my mentor, Sheldon Friedman, and his wife, Rita Friedman (Rosenzweig), who chose to invest in my success at a young age. I have only made it this far thanks to their undying encouragement, love, and optimism. To Sheldon's best friend, Dr. Bernard Khoury, whose reputation and has helped pave my own path. To the many moms who generously gave unconditional support during the darkest of times and unequivocal love during the brightest times: Cyndi Reilly-Rogers, Dawn Hood, Margaret Sherrill, and Silet Wiley.

To Dr. Filippo Errico for his focus, leadership, selflessness, and patience in leading the Higgs mass analysis. To Dr. Lucien Lo for showing me the simplicity and beauty of Python in his typical laid-back way and for leading the dilepton analysis. To Dr. Noah Steinberg for showing me how majestically physics can be communicated from mind to mind. To Dr. Darin Acosta, for spending many hours of physics discussion with me and the other students, who have helped us build our "CMS Office Hours" Ari Gonzalez, Cris Caballeros, Jeremiah Anglin, Sean Kent, Evan Koenig, Neha Rawal, Nik Menendez, John Rötter. To the gents who paved my way to and through the world of CMS, Brendan Regnery and Bhargav Joshi. To my mentee, Matthew Dittrich, for accepting the baton of knowledge and making everything come full circle.

To my comrades for showing me what it takes to survive the core courses, Dr. Atoul Divakarla, Dr. Brien O'Brendan, Dr. Donyell Guerrero, and Dr. Vladinar Martinez. To Adamya Goyal for all his gentleness, humility, patience, and tutorage. To my Polish roommates in Saint-Genis-Pouilly for showing me what home away from home feels like: Bartoszek, Dziadzius,

Karolina, and Sandruša. To the boys who have been there since the beginning: Jish, Willis, The Shane, Zacman, Duck, and Marcus for their clever competition and continual camaraderie which has shaped me to this day.

To Big Tree who stood as a symbol of strength, beauty, and life for centuries before us. As Irma's wild whirring winds worsened, the cacophony of ripping roots resounded throughout the western corridor. There I stood in that frozen moment—awestruck, speechless—watching her *fall* helplessly towards the physics building. What could have been a catastrophe of cataclysmic proportions was instead a gentle grazing against the north windows of NPB where, there, she was gracefully laid to rest.

Finally, to Existence, for this unpredictable, unbelievable blip of an experience called Life.

TABLE OF CONTENTS

	<u>page</u>
ACKNOWLEDGEMENTS	4
LIST OF TABLES	7
LIST OF FIGURES	8
ABSTRACT	9
CHAPTER	
1 HIGGS BOSON MASS MEASUREMENT IN THE $H \rightarrow ZZ^* \rightarrow 4\ell$ CHANNEL	10
1.1 Motivation	10
1.2 Analyzed Data	12
1.2.1 Triggers	12
1.2.2 Data Sets	12
1.2.3 Simulated Events	12
1.2.4 PileUp reweight	12
2 SEARCH FOR LOW-MASS DILEPTON RESONANCES IN THE $H \rightarrow 4\ell$ CHANNEL .	21
2.1 Motivation	21
2.2 Overview	21
2.3 Results	23
REFERENCES	26
BIOGRAPHICAL SKETCH	28

LIST OF TABLES

<u>Tables</u>	<u>page</u>
1-1 Trigger paths used to collect 2016 data (pre- and post-VFP)	13
1-2 Trigger paths used to collect 2017 data	14
1-3 Trigger paths used to collect 2018 data	14
1-4 Data sets used for 2016 UL	15
1-5 UL data sets used for 2017	16
1-6 UL data sets used for 2018	16
1-7 Names of simulated signal and background samples for 2016 data.	17
1-8 Names of simulated signal and background samples for 2017 data.	17
1-9 Names of simulated signal and background samples for 2018 data.	18

LIST OF FIGURES

<u>Figures</u>	<u>page</u>
1-1 Various measurements of m_H made by the CMS and ATLAS collaborations.	11
1-2 words	20
2-1 Exotic decays of the Higgs boson to the 4ℓ final state.....	22
2-2 test.....	23

Abstract of Dissertation Presented to the Graduate School
of the University of Florida in Partial Fulfillment of the
Requirements for the Degree of Doctor of Philosophy

PRECISION MEASUREMENT OF THE HIGGS BOSON MASS AND SEARCH FOR
DILEPTON MASS RESONANCES IN $H \rightarrow 4\ell$ DECAYS USING THE CMS DETECTOR AT
THE LHC

By

Jake Rosenzweig

December 2022

Chair: Andrey Korytov

Co-Chair: Guenakh Mitselmakher

Major: Physics

The mass of the Higgs boson is measured in the $H \rightarrow ZZ^* \rightarrow 4\ell$ ($\ell = e, \mu$) decay channel and is found to be $m_H = 125.38 \pm 0.11$ GeV; the most precise measurement of m_H in the world to date. The data for the measurement were produced from proton-proton (pp) collisions at the Large Hadron Collider with a center-of-mass energy of 13 TeV during Run 2 (2016–2018), corresponding to an integrated luminosity of 137.1 fb^{-1} , and were collected by the Compact Muon Solenoid experiment. This measurement uses an improved analysis technique in which the final state muon tracks are constrained to originate from the primary pp vertex. Using data sets from the same run, a search for low-mass dilepton resonances in Higgs boson decays to the 4ℓ final state is also conducted. No significant deviation from the Standard Model prediction is observed.

CHAPTER 1

HIGGS BOSON MASS MEASUREMENT IN THE $H \rightarrow ZZ^* \rightarrow 4\ell$ CHANNEL

1.1 Motivation

When the CMS and ATLAS collaborations announced the discovery of the Higgs boson on July 4, 2012, this was a momentous achievement in particle physics because the so-called “missing” piece of the SM was found. Evidence of the Higgs boson’s existence also motivates the associated Higgs field, which permeates all of spacetime and explains the origins of the masses of all the other massive fundamental particles (Chapter ??).

The Higgs boson is interesting for a variety of reasons. First, it is currently one of a kind—the only fundamental scalar particle ever discovered at the time of this writing. Second, the mass of the Higgs boson theoretically determines the stability of our very Universe (Fig. ??). Third, the unique boson could be a portal to new physics—i.e., physics beyond the Standard Model (BSM)—e.g., by decaying into BSM low-mass dilepton mass resonances (Chapter 2). Fourth, the Higgs boson may not be the only one of its kind; some BSM models theorize that other kinds of Higgs bosons may exist. Fifth, *are we certain that the Higgs boson discovered in 2012 is the same as the one predicted by the SM?* To check this, it is necessary to compare the Higgs boson’s measured properties to its predicted ones. One such property is the mass of the Higgs boson (m_H).

This chapter details the measurement of m_H full Run 2 data from the LHC as analyzed by the CMS detector. Although many previous measurements of m_H have already been made (e.g., by the ATLAS and CMS collaborations as shown in Fig. 1-1), the measurement presented in this dissertation gives the world’s most precise value of m_H .

First, a general overview of the logic and analysis workflow for the m_H measurement is motivated in Sec. ??. The specific data sets, simulated samples, and triggers used in the analysis are then detailed in Sec. 1.2. Then the event reconstruction and event selection are described in Sec. ??. Afterwards, an analysis of the background estimation is given in Sec. ??. The signal modeling and improvements utilized in this measurement are then laid out, which include the kinematic discriminant, per-event mass uncertainties, and the vertex constraint in Sec. ??. A treatment of the systematic uncertainties follows in Sec. ??. The chapter concludes with a summary of the m_H measurement results in Sec. ??.

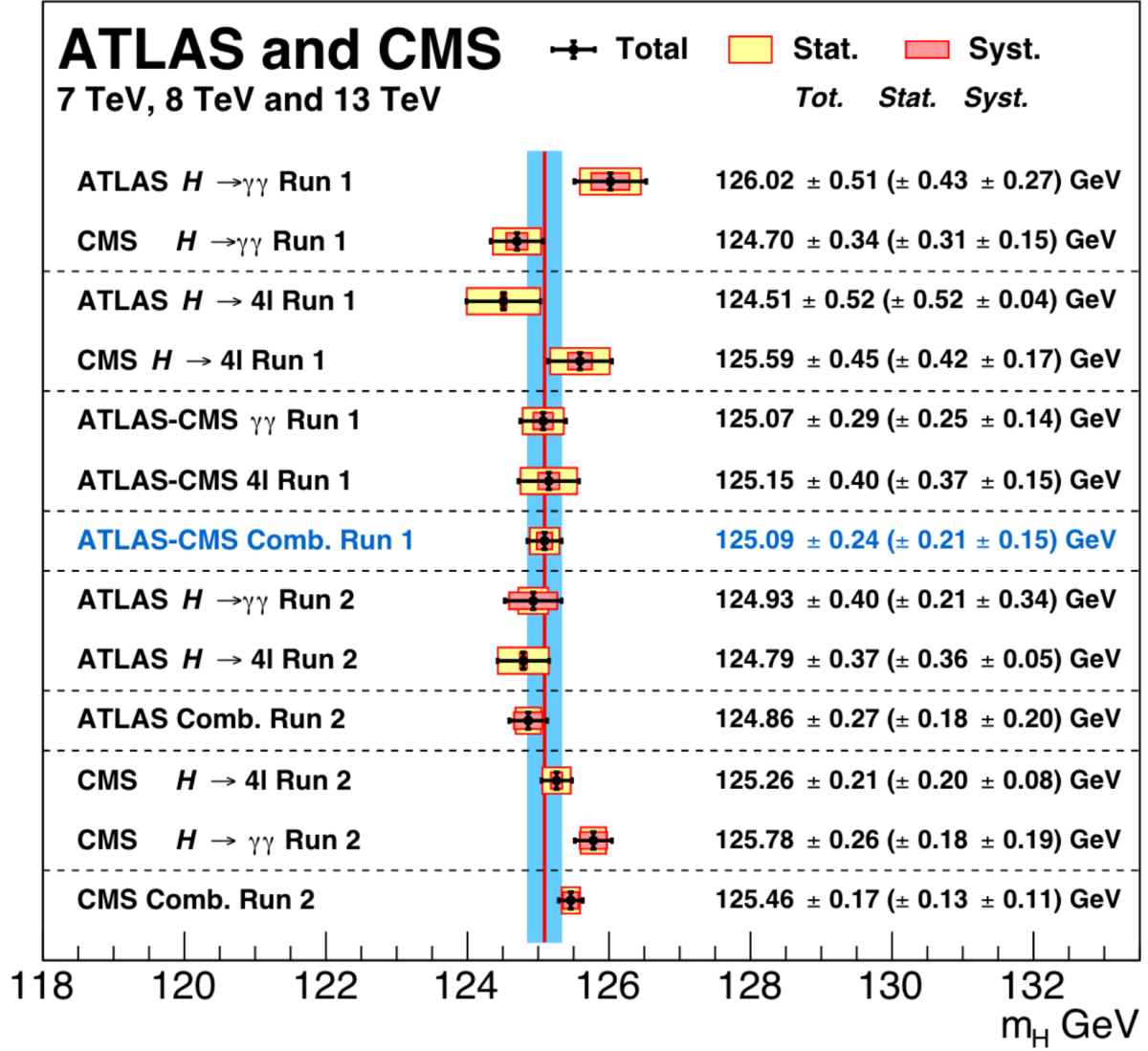


Figure 1-1. Various measurements of m_H made by the CMS and ATLAS collaborations in the $H \rightarrow \gamma\gamma$ and $H \rightarrow ZZ^* \rightarrow 4\ell$ channels, in Runs 1 and 2 of the LHC. Plot taken from [1].

1.2 Analyzed Data

The CMS experiment recorded LHC data during 2016, 2017, and 2018 (collectively called Run 2), corresponding to an integrated luminosity of 137.1 fb^{-1} . These events were categorized by the trigger system into different data sets, depending on which triggers “fired”, i.e., whether the event passed the trigger criteria or not. The names of the data sets are listed in Tables 1-4–1-6 and follow the format /object_type/campaign/datatier. This analysis uses the ultra legacy (UL) reconstruction []. It should be noted that the 2016 data are split into 2 different reconstruction versions, starting at Run2016F: the first version is “pre-VFP”, which uses HIP mitigation (HIPM) in the reconstruction, and the second is “post-VFP”, which uses the default reconstruction.

For the $H \rightarrow ZZ^* \rightarrow 4\ell$ analysis, Sec. 1.2.1 lists the triggers used, Sec. 1.2.2 details the data sets used, and Sec. 1.2.3 summarizes the simulated samples used.

1.2.1 Triggers

1.2.2 Data Sets

1.2.3 Simulated Events

The data set names containing the simulated events for signal and background processes are listed in Tables 1-7–1-9.

1.2.4 PileUp reweight

Simulated samples are reweighted taking into account pileUp distribution. PileUp weight is extracted for each year matching simulation and data distribution. The minimum bias cross-section used for each year is 69.2 mb . PileUp distributions for each year are shown in Fig. 1-2.

Table 1-1. Trigger paths used to collect 2016 data (pre- and post-VFP) for the measurement of m_H .

HLT path	Prescale	Primary data set
HLT_DoubleEle33_CaloIdL_GsfTrkIdVL_v*	1	DoubleEG
HLT_Ele16_Ele12_Ele8_CaloIdL_TrackIdL_v*	1	DoubleEG
HLT_Ele17_Ele12_CaloIdL_TrackIdL_IsoVL_DZ_v*	1	DoubleEG
HLT_Ele23_Ele12_CaloIdL_TrackIdL_IsoVL_DZ_v*	1	DoubleEG
HLT_Mu17_TrkIsoVVL_Mu8_TrkIsoVVL_DZ_v*	1	DoubleMuon
HLT_Mu17_TrkIsoVVL_Mu8_TrkIsoVVL_v*	1	DoubleMuon
HLT_Mu17_TrkIsoVVL_TkMu8_TrkIsoVVL_DZ_v*	1	DoubleMuon
HLT_Mu17_TrkIsoVVL_TkMu8_TrkIsoVVL_v*	1	DoubleMuon
HLT_TripleMu_12_10_5_v*	1	DoubleMuon
HLT_DiMu9_Ele9_CaloIdL_TrackIdL_v*	1	MuonEG
HLT_Mu8_DiEle12_CaloIdL_TrackIdL_v*	1	MuonEG
HLT_Mu8_TrkIsoVVL_Ele17_CaloIdL_TrackIdL_IsoVL_v*	1	MuonEG
HLT_Mu8_TrkIsoVVL_Ele23_CaloIdL_TrackIdL_IsoVL_DZ_v*	1	MuonEG
HLT_Mu8_TrkIsoVVL_Ele23_CaloIdL_TrackIdL_IsoVL_v*	1	MuonEG
HLT_Mu17_TrkIsoVVL_Ele12_CaloIdL_TrackIdL_IsoVL_v*	1	MuonEG
HLT_Mu23_TrkIsoVVL_Ele8_CaloIdL_TrackIdL_IsoVL_v*	1	MuonEG
HLT_Mu23_TrkIsoVVL_Ele12_CaloIdL_TrackIdL_IsoVL_DZ_v*	1	MuonEG
HLT_Mu23_TrkIsoVVL_Ele12_CaloIdL_TrackIdL_IsoVL_v*	1	MuonEG
HLT_Ele25_eta2p1_WPTight_Gsf_v*	1	SingleElectron
HLT_Ele27_eta2p1_WPLoose_Gsf_v*	1	SingleElectron
HLT_Ele27_WPTight_Gsf_v*	1	SingleElectron
HLT_Ele32_eta2p1_WPTight_Gsf_v*	1	SingleElectron
HLT_IsoMu20_v* OR HLT_IsoTkMu20_v*	1	SingleMuon
HLT_IsoMu22_v* OR HLT_IsoTkMu22_v*	1	SingleMuon
HLT_IsoMu24_v* OR HLT_IsoTkMu24_v*	1	SingleMuon

Table 1-2. Trigger paths used to collect 2017 data for the measurement of m_H .

HLT path	Prescale	Primary data set
HLT_DoubleEle33_CaloIdL_MW_v*	1	DoubleEG
HLT_Ele16_Ele12_Ele8_CaloIdL_TrackIdL_v*	1	DoubleEG
HLT_Ele23_Ele12_CaloIdL_TrackIdL_IsoVL_v*	1	DoubleEG
HLT_Mu17_TrkIsoVVL_Mu8_TrkIsoVVL_DZ_Mass3p8_v*	1	DoubleMuon
HLT_Mu17_TrkIsoVVL_Mu8_TrkIsoVVL_DZ_Mass8_v*	1	DoubleMuon
HLT_TripleMu_10_5_5_DZ_v*	1	DoubleMuon
HLT_TripleMu_12_10_5_v*	1	DoubleMuon
HLT_DiMu9_Ele9_CaloIdL_TrackIdL_DZ_v*	1	MuonEG
HLT_Mu8_DiEle12_CaloIdL_TrackIdL_DZ_v*	1	MuonEG
HLT_Mu8_DiEle12_CaloIdL_TrackIdL_v*	1	MuonEG
HLT_Mu8_TrkIsoVVL_Ele23_CaloIdL_TrackIdL_IsoVL_DZ_v*	1	MuonEG
HLT_Mu12_TrkIsoVVL_Ele23_CaloIdL_TrackIdL_IsoVL_DZ_v*	1	MuonEG
HLT_Mu23_TrkIsoVVL_Ele12_CaloIdL_TrackIdL_IsoVL_DZ_v*	1	MuonEG
HLT_Mu23_TrkIsoVVL_Ele12_CaloIdL_TrackIdL_IsoVL_v*	1	MuonEG
HLT_Ele35_WPTight_Gsf_v*	1	SingleElectron
HLT_Ele38_WPTight_Gsf_v*	1	SingleElectron
HLT_Ele40_WPTight_Gsf_v*	1	SingleElectron
HLT_IsoMu27_v*	1	SingleMuon

Table 1-3. Trigger paths used to collect 2018 data for the measurement of m_H .

HLT path	Prescale	Primary data set
HLT_DoubleEle25_CaloIdL_MW_v*	1	DoubleEG
HLT_Ele23_Ele12_CaloIdL_TrackIdL_IsoVL_v*	1	DoubleEG
HLT_Mu17_TrkIsoVVL_Mu8_TrkIsoVVL_DZ_Mass3p8_v*	1	DoubleMuon
HLT_TripleMu_10_5_5_DZ_v*	1	DoubleMuon
HLT_TripleMu_12_10_5_v*	1	DoubleMuon
HLT_DiMu9_Ele9_CaloIdL_TrackIdL_DZ_v*	1	MuonEG
HLT_Mu8_DiEle12_CaloIdL_TrackIdL_DZ_v*	1	MuonEG
HLT_Mu8_DiEle12_CaloIdL_TrackIdL_v*	1	MuonEG
HLT_Mu8_TrkIsoVVL_Ele23_CaloIdL_TrackIdL_IsoVL_DZ_v*	1	MuonEG
HLT_Mu12_TrkIsoVVL_Ele23_CaloIdL_TrackIdL_IsoVL_DZ_v*	1	MuonEG
HLT_Mu23_TrkIsoVVL_Ele12_CaloIdL_TrackIdL_IsoVL_DZ_v*	1	MuonEG
HLT_Mu23_TrkIsoVVL_Ele12_CaloIdL_TrackIdL_IsoVL_v*	1	MuonEG
HLT_Ele32_WPTight_Gsf_v*	1	SingleElectron
HLT_IsoMu24_v*	1	SingleMuon

Table 1-4. Names of the UL 2016 data sets and the corresponding integrated luminosities (\mathcal{L}_{int}).

Data set name	Integrated luminosity (fb^{-1})
/DoubleEG/Run2016B-ver1_HIPM_UL2016_MiniAODv2-v1/MINIAOD /DoubleMuon/Run2016B-ver1_HIPM_UL2016_MiniAODv2-v1/MINIAOD /SingleElectron/Run2016B-ver1_HIPM_UL2016_MiniAODv2-v2/MINIAOD /SingleMuon/Run2016B-ver1_HIPM_UL2016_MiniAODv2-v2/MINIAOD /MuonEG/Run2016B-ver1_HIPM_UL2016_MiniAODv2-v2/MINIAOD	TODO
/DoubleEG/Run2016B-ver2_HIPM_UL2016_MiniAODv2-v3/MINIAOD /DoubleMuon/Run2016B-ver2_HIPM_UL2016_MiniAODv2-v1/MINIAOD /SingleElectron/Run2016B-ver2_HIPM_UL2016_MiniAODv2-v2/MINIAOD /SingleMuon/Run2016B-ver2_HIPM_UL2016_MiniAODv2-v2/MINIAOD /MuonEG/Run2016B-ver2_HIPM_UL2016_MiniAODv2-v2/MINIAOD	TODO
/DoubleEG/Run2016C-HIPM_UL2016_MiniAODv2-v1/MINIAOD /DoubleMuon/Run2016C-HIPM_UL2016_MiniAODv2-v1/MINIAOD /SingleElectron/Run2016C-HIPM_UL2016_MiniAODv2-v2/MINIAOD /SingleMuon/Run2016C-HIPM_UL2016_MiniAODv2-v2/MINIAOD /MuonEG/Run2016C-HIPM_UL2016_MiniAODv2-v2/MINIAOD	TODO
/DoubleEG/Run2016D-HIPM_UL2016_MiniAODv2-v1/MINIAOD /DoubleMuon/Run2016D-HIPM_UL2016_MiniAODv2-v1/MINIAOD /SingleElectron/Run2016D-HIPM_UL2016_MiniAODv2-v2/MINIAOD /SingleMuon/Run2016D-HIPM_UL2016_MiniAODv2-v2/MINIAOD /MuonEG/Run2016D-HIPM_UL2016_MiniAODv2-v2/MINIAOD	TODO
/DoubleEG/Run2016E-HIPM_UL2016_MiniAODv2-v1/MINIAOD /DoubleMuon/Run2016E-HIPM_UL2016_MiniAODv2-v1/MINIAOD /SingleElectron/Run2016E-HIPM_UL2016_MiniAODv2-v5/MINIAOD /SingleMuon/Run2016E-HIPM_UL2016_MiniAODv2-v2/MINIAOD /MuonEG/Run2016E-HIPM_UL2016_MiniAODv2-v2/MINIAOD	TODO
/DoubleEG/Run2016F-HIPM_UL2016_MiniAODv2-v1/MINIAOD /DoubleMuon/Run2016F-HIPM_UL2016_MiniAODv2-v1/MINIAOD /SingleElectron/Run2016F-HIPM_UL2016_MiniAODv2-v2/MINIAOD /SingleMuon/Run2016F-HIPM_UL2016_MiniAODv2-v2/MINIAOD /MuonEG/Run2016F-HIPM_UL2016_MiniAODv2-v2/MINIAOD	TODO
/DoubleEG/Run2016F-UL2016_MiniAODv2-v1/MINIAOD /DoubleMuon/Run2016F-UL2016_MiniAODv2-v1/MINIAOD /SingleElectron/Run2016F-UL2016_MiniAODv2-v2/MINIAOD /SingleMuon/Run2016F-UL2016_MiniAODv2-v2/MINIAOD /MuonEG/Run2016F-UL2016_MiniAODv2-v2/MINIAOD	TODO
/DoubleEG/Run2016G-UL2016_MiniAODv2-v1/MINIAOD /DoubleMuon/Run2016G-UL2016_MiniAODv2-v1/MINIAOD /SingleElectron/Run2016G-UL2016_MiniAODv2-v2/MINIAOD /SingleMuon/Run2016G-UL2016_MiniAODv2-v2/MINIAOD /MuonEG/Run2016G-UL2016_MiniAODv2-v2/MINIAOD	TODO
/DoubleEG/Run2016H-UL2016_MiniAODv2-v1/MINIAOD /DoubleMuon/Run2016H-UL2016_MiniAODv2-v2/MINIAOD /SingleElectron/Run2016H-UL2016_MiniAODv2-v2/MINIAOD /SingleMuon/Run2016H-UL2016_MiniAODv2-v2/MINIAOD /MuonEG/Run2016H-UL2016_MiniAODv2-v2/MINIAOD	TODO

Table 1-5. Names of the UL 2017 data sets and the corresponding integrated luminosities (\mathcal{L}_{int}).

Data set name	Integrated luminosity (fb^{-1})
/SingleMuon/Run2017B-UL2017_MiniAODv2-v1/MINIAOD /SingleElectron/Run2017B-UL2017_MiniAODv2-v1/MINIAOD /DoubleMuon/Run2017B-UL2017_MiniAODv2-v1/MINIAOD /DoubleEG/Run2017B-UL2017_MiniAODv2-v1/MINIAOD /MuonEG/Run2017B-UL2017_MiniAODv2-v1/MINIAOD	TODO
/SingleMuon/Run2017C-UL2017_MiniAODv2-v1/MINIAOD /SingleElectron/Run2017C-UL2017_MiniAODv2-v1/MINIAOD /DoubleMuon/Run2017C-UL2017_MiniAODv2-v1/MINIAOD /DoubleEG/Run2017C-UL2017_MiniAODv2-v1/MINIAOD /MuonEG/Run2017C-UL2017_MiniAODv2-v1/MINIAOD	TODO
/SingleElectron/Run2017D-UL2017_MiniAODv2-v1/MINIAOD /SingleMuon/Run2017D-UL2017_MiniAODv2-v1/MINIAOD /DoubleMuon/Run2017D-UL2017_MiniAODv2-v1/MINIAOD /DoubleEG/Run2017D-UL2017_MiniAODv2-v1/MINIAOD /MuonEG/Run2017D-UL2017_MiniAODv2-v1/MINIAOD	TODO
/SingleElectron/Run2017E-UL2017_MiniAODv2-v1/MINIAOD /SingleMuon/Run2017E-UL2017_MiniAODv2-v1/MINIAOD /DoubleMuon/Run2017E-UL2017_MiniAODv2-v2/MINIAOD /DoubleEG/Run2017E-UL2017_MiniAODv2-v1/MINIAOD /MuonEG/Run2017E-UL2017_MiniAODv2-v1/MINIAOD	TODO
/SingleElectron/Run2017F-UL2017_MiniAODv2-v1/MINIAOD /SingleMuon/Run2017F-UL2017_MiniAODv2-v1/MINIAOD /DoubleMuon/Run2017F-UL2017_MiniAODv2-v1/MINIAOD /DoubleEG/Run2017F-UL2017_MiniAODv2-v1/MINIAOD /MuonEG/Run2017F-UL2017_MiniAODv2-v1/MINIAOD	TODO

Table 1-6. Names of the UL 2018 data sets and the corresponding integrated luminosities (\mathcal{L}_{int}).

Data set name	Integrated luminosity (fb^{-1})
/SingleMuon/Run2018A-UL2018_MiniAODv2-v3/MINIAOD /DoubleMuon/Run2018A-UL2018_MiniAODv2-v1/MINIAOD /EGamma/Run2018A-UL201_MiniAODv2-v1/MINIAOD /MuonEG/Run2018A-UL2018_MiniAODv2-v1/MINIAOD	TODO
/SingleMuon/Run2018B-UL2018_MiniAODv2-v2/MINIAOD /DoubleMuon/Run2018B-UL2018_MiniAODv2-v1/MINIAOD /EGamma/Run2018B-UL2018_MiniAODv2-v1/MINIAOD /MuonEG/Run2018B-UL2018_MiniAODv2-v1/MINIAOD	TODO
/SingleMuon/Run2018C-UL2018_MiniAODv2-v2/MINIAOD /DoubleMuon/Run2018C-UL2018_MiniAODv2-v1/MINIAOD /EGamma/Run2018C-UL2018_MiniAODv2-v1/MINIAOD /MuonEG/Run2018C-UL2018_MiniAODv2-v1/MINIAOD	TODO
/SingleMuon/Run2018D-UL2018_MiniAODv2-v3/MINIAOD /DoubleMuon/Run2018D-UL2018_MiniAODv2-v1/MINIAOD /EGamma/Run2018D-UL2018_MiniAODv2-v1/MINIAOD /MuonEG/Run2018D-UL2018_MiniAODv2-v1/MINIAOD	TODO

Table 1-7. Names of simulated signal and background samples for 2016 data.

[1] “RunIISummer20UL16MiniAODv2-106X_mcRun2_asymptotic_v17-v2/MINIAODSIM”

or

“RunIISummer20UL16MiniAODAPV2-106X_mcRun2_asymptotic_preVFP_v11-v2/MINIAODSIM”

Name of signal data set	$\sigma \times \mathcal{B}$ (pb)
GluGluHToZZTo4L_M125_13TeV_powheg2_JHUGenV709_pythia8/[1]	0.01333521
VBF_HTToZZTo4L_M125_13TeV_powheg2_JHUGenV709_pythia8/[1]	0.001038159
WplusH_HTToZZTo4L_M125_13TeV_powheg2-minlo-HWJ_JHUGenV709_pythia8/[1]	0.0002305562
WminusH_HTToZZTo4L_M125_13TeV_powheg2-minlo-HWJ_JHUGenV709_pythia8/[1]	0.0001462348
ZH_HTToZZ_4LFilter_M125_13TeV_powheg2-minlo-HZJ_JHUGenV709_pythia8/[1]	0.0005321759
ttH_HTToZZ_4LFilter_M125_13TeV_powheg2_JHUGenV709_pythia8/[1]	0.0003639351
bbH_HTToZZTo4L_M125_13TeV_JHUGenV702_pythia8/[1]	0.0001339560
tqH_HTToZZTo4L_M125_TuneCP5_13TeV-jhugenv7011pythia8/[1]	0.0000857830
Name of background data set	$\sigma \times \mathcal{B}$ (pb)
ZZTo4L_13TeV_powheg_pythia8/[1]	1.256
GluGluToContinToZZTo4e_13TeV_MCFM701_pythia8/[1]	0.00158549
GluGluToContinToZZTo4mu_13TeV_MCFM701_pythia8/[1]	0.00158549
GluGluToContinToZZTo4tau_13TeV_MCFM701_pythia8/[1]	0.00158549
GluGluToContinToZZTo2e2mu_13TeV_MCFM701_pythia8/[1]	0.0031942
GluGluToContinToZZTo2e2tau_13TeV_MCFM701_pythia8/[1]	0.0031942
GluGluToContinToZZTo2mu2tau_13TeV_MCFM701_pythia8/[1]	0.0031942

Table 1-8. Names of simulated signal and background samples for 2017 data.

[2] “RunIISummer20UL17MiniAODv2-106X_mc2017_realistic_v9/MINIAODSIM”

Name of signal data set	$\sigma \times \mathcal{B}$ (pb)
GluGluHToZZTo4L_M125_13TeV_powheg2_JHUGenV7011_pythia8/[2]	0.01333521
VBF_HTToZZTo4L_M125_13TeV_powheg2_JHUGenV7011_pythia8/[2]	0.001038159
WplusH_HTToZZTo4L_M125_13TeV_powheg2-minlo-HWJ_JHUGenV7011_pythia8/[2]	0.0002305562
WminusH_HTToZZTo4L_M125_13TeV_powheg2-minlo-HWJ_JHUGenV7011_pythia8/[2]	0.0001462348
ZH_HTToZZ_4LFilter_M125_13TeV_powheg2-minlo-HZJ_JHUGenV7011_pythia8/[2]	0.0005321759
ttH_HTToZZ_4LFilter_M125_13TeV_powheg2_JHUGenV7011_pythia8/[2]	0.0003639351
bbH_HTToZZTo4L_M125_13TeV_JHUGenV7011_pythia8/[2]	0.0001339560
tqH_HTToZZTo4L_M125_TuneCP5_13TeV-jhugenv7011pythia8/[1]	0.0000857830
Name of background data set	$\sigma \times \mathcal{B}$ (pb)
ZZTo4L_13TeV_powheg_pythia8/[2]	1.256
GluGluToContinToZZTo4e_13TeV_MCFM701_pythia8/[2]	0.00158549
GluGluToContinToZZTo4mu_13TeV_MCFM701_pythia8/[2]	0.00158549
GluGluToContinToZZTo4tau_13TeV_MCFM701_pythia8/[2]	0.00158549
GluGluToContinToZZTo2e2mu_13TeV_MCFM701_pythia8/[2]	0.0031942
GluGluToContinToZZTo2e2tau_13TeV_MCFM701_pythia8/[2]	0.0031942
GluGluToContinToZZTo2mu2tau_13TeV_MCFM701_pythia8/[2]	0.0031942

Table 1-9. Names of simulated signal and background samples for 2018 data.

[3] “RunIISummer20UL18MiniAODv2-
106X_upgrade2018_realistic_v16_L1v1/MINIAODSIM”

Name of signal data set	$\sigma \times \mathcal{B}$ (pb)
GluGluHToZZTo4L_M125_13TeV_powheg2_JHUGenV7011_pythia8/[3]	0.01333521
VBF_HToZZTo4L_M125_13TeV_powheg2_JHUGenV7011_pythia8/[3]	0.001038159
WplusH_HToZZTo4L_M125_13TeV_powheg2-minlo-HWJ_JHUGenV7011_pythia8/[3]	0.0002305562
WminusH_HToZZTo4L_M125_13TeV_powheg2-minlo-HWJ_JHUGenV7011_pythia8/[3]	0.0001462348
ZH_HToZZ_4LFilter_M125_13TeV_powheg2-minlo-HZJ_JHUGenV7011_pythia8/[3]	0.0005321759
ttH_HToZZ_4LFilter_M125_13TeV_powheg2_JHUGenV7011_pythia8/[3]	0.0003639351
bbH_HToZZTo4L_M125_TuneCP2_13TeV-JHUGenV7011_pythia8/[3]	0.0001339560
tqH_HToZZTo4L_M125_TuneCP5_13TeV-jhugenv7011pythia8/[1]	0.0000857830
Name of background data set	$\sigma \times \mathcal{B}$ (pb)
ZZTo4L_TuneCP5_13TeV_powheg_pythia8/[3]	1.256
GluGluToContinToZZTo4e_13TeV_MCFM701_pythia8/[3]	0.00158549
GluGluToContinToZZTo4mu_13TeV_MCFM701_pythia8/[3]	0.00158549
GluGluToContinToZZTo4tau_13TeV_MCFM701_pythia8/[3]	0.00158549
GluGluToContinToZZTo2e2mu_13TeV_MCFM701_pythia8/[3]	0.0031942
GluGluToContinToZZTo2e2tau_13TeV_MCFM701_pythia8/[3]	0.0031942
GluGluToContinToZZTo2mu2tau_13TeV_MCFM701_pythia8/[3]	0.0031942

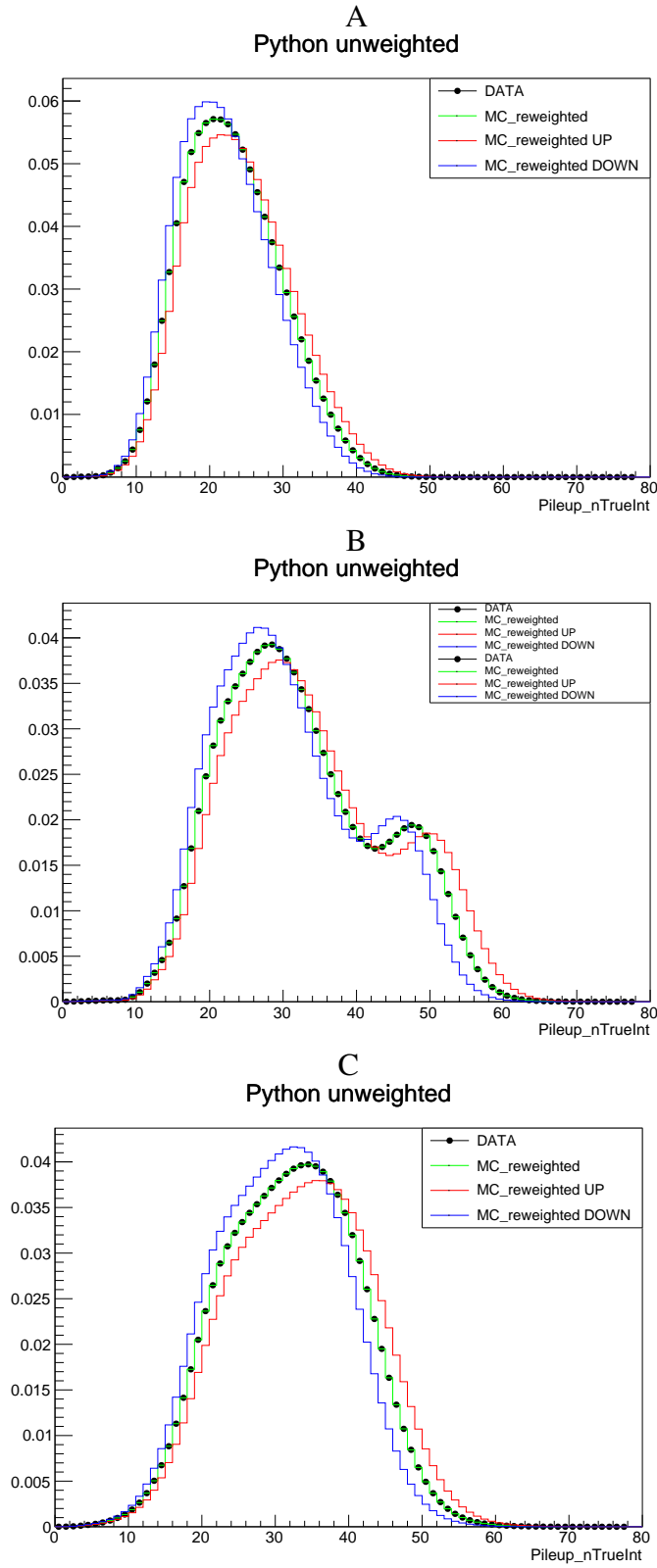


Figure 1-2. TODO:REWORD Data–simulation pileUp distributions: left 2016 (for pre and post-VFP), right 2017, bottom 2018. Up (down) scale has been obtained using 72.4 (66)mb.

CHAPTER 2

SEARCH FOR LOW-MASS DILEPTON RESONANCES IN THE $H \rightarrow 4\ell$ CHANNEL

2.1 Motivation

As mentioned in Sec. 1.1, even though the Higgs boson has been well studied and *appears* to be consistent with the SM Higgs boson, a single experiment that shows BSM activity (i.e., *any* deviation from SM prediction) is all that is required to completely defenestrate this idea. For example, it may be the case that the Higgs boson (H) decays into particles other than those found in the SM. This chapter details such an analysis, which follows similar topologies to the one studied in Chapter 1 ($H \rightarrow ZZ^* \rightarrow 4\ell$), specifically $H \rightarrow ZX \rightarrow 4\ell$ and $H \rightarrow XX \rightarrow 4\ell$, where X is a BSM low-mass dilepton resonance.

2.2 Overview

This analysis searches for exotic decays of the Higgs boson (H) using data collected by the CMS experiment (Chapter ??) from the pp collisions produced at the CERN LHC (Chapter ??) at a center-of-mass energy of 13 TeV during the Run 2 period (2016–2018). Two different decay mechanisms are considered: $H \rightarrow ZX$ and $H \rightarrow XX$. Here, X represents a BSM particle that may decay into a pair of OSSF leptons, though only electrons and muons are considered. Because the Z is the SM Z boson, this decay process yields the same four-lepton (4ℓ) final states that were found in the Higgs boson mass measurement analysis (Chapter 1): $4e$, 4μ , $2e2\mu$, and $2\mu2e$. The 4ℓ final state was chosen due to its clean signature and large signal-to-background ratio.

Not only is X a theoretical BSM particle, it is speculated to interact with SM particles via the “dark” sector. Such dark sector particles are described within the theoretical framework of the “hidden Abelian Higgs model” (HAHM) TODO:refs7–11 from EJPC. Within the context of the HAHM, X is the dark photon (Z_D). This dark particle mediates a dark $U(1)_D$ gauge symmetry that is spontaneously broken by a theoretical dark Higgs mechanism.

The search for Z_D begins with a SM decay of $H \rightarrow ZZ$. Then, via the dark sector, one of the Z bosons *mixes* with Z_D , as determined by the kinetic-mixing parameter ε . The Z_D and the other Z then decay into OSSF lepton pairs to yield one of the four different 4ℓ final states. This decay process is shown in Fig. 2-1 (Left). The other mode of Z_D production occurs when a H mixes with a dark Higgs boson (s), as governed by the Higgs-mixing parameter κ . Then, the s decays into two

identical Z_D particles which decay promptly to give one of the 4ℓ final states. This decay process is shown in Fig. 2-1 (Right).

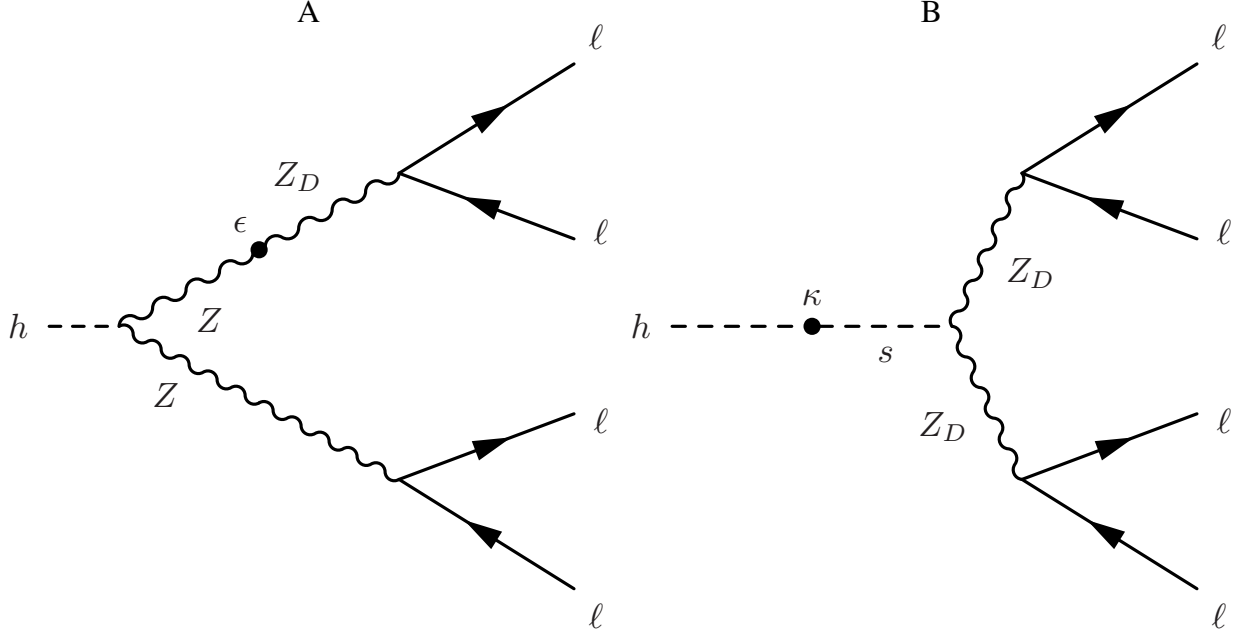


Figure 2-1. Exotic decays of the Higgs boson (h) to the 4ℓ final state within the context of the HAHM. A) Higgs boson decays into two SM Z bosons, one of which kinetically mixes with the dark photon (Z_D). B) Higgs boson mixes with a dark Higgs boson (s) via the Higgs-mixing mechanism, governed by the Higgs-mixing parameter κ . The dark Higgs then decays into two identical dark photons, each of which decays into two OSSF leptons.

This analysis assumes a narrow-width approximation for Z_D decays so that the dark photon is confined to its on-mass shell. Thus, for any given dark photon mass hypothesis, Z_D is assumed to always have that singular mass value. This limitation on the mass of Z_D (m_{Z_D}) in conjunction with the narrow-width nature of the Higgs boson mass resonance ($m_H \approx 125 \text{ GeV}$) kinematically constrains the search region of the analysis. Specifically, the $H \rightarrow ZZ_D$ ($H \rightarrow Z_D Z_D$) process has the upper limit $m_{Z_D} < m_H - m_Z \approx 35 \text{ GeV}$ ($m_{Z_D} < m_H/2 \approx 62.5 \text{ GeV}$). Finally, to avoid the ubiquitous but unwanted reconstruction of an intermediate J/ψ ($c\bar{c}$) meson, which has a precisely measured mass of $3.096900 \pm 0.000006 \text{ GeV}$ [1], the mass range chosen for this analysis is $4.0 < m_{Z_D} < 35.0 \text{ GeV}$ (62.5 GeV).

This low-mass dilepton resonance search has a similar to the aforementioned Higgs boson mass measurement analysis described in

2.3 Results

CL_s [2].

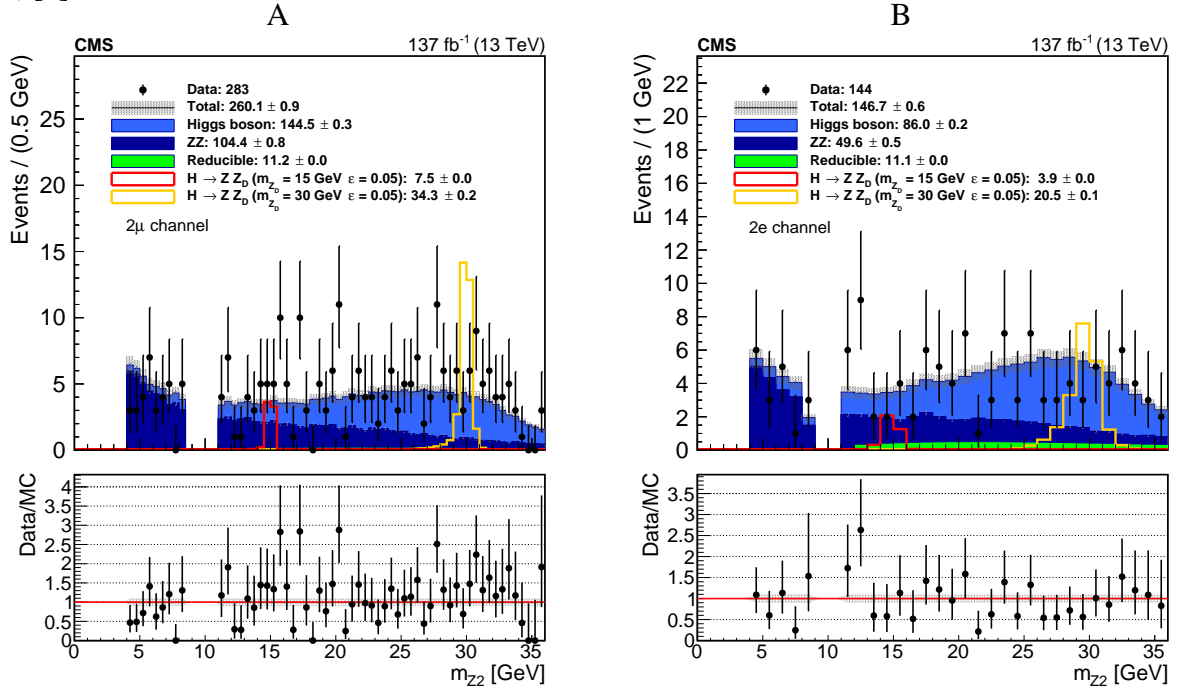
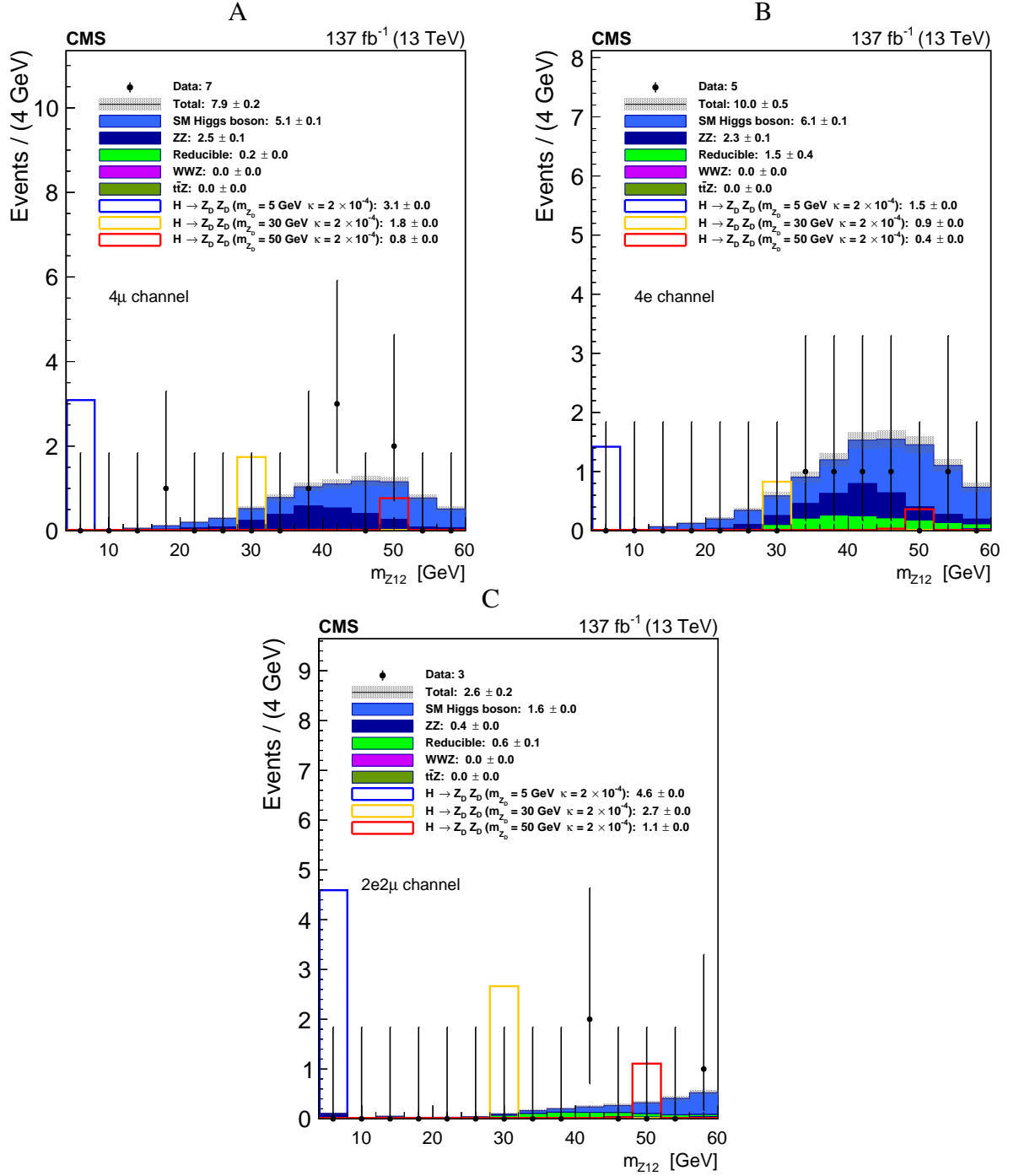


Figure 2-2. testing more



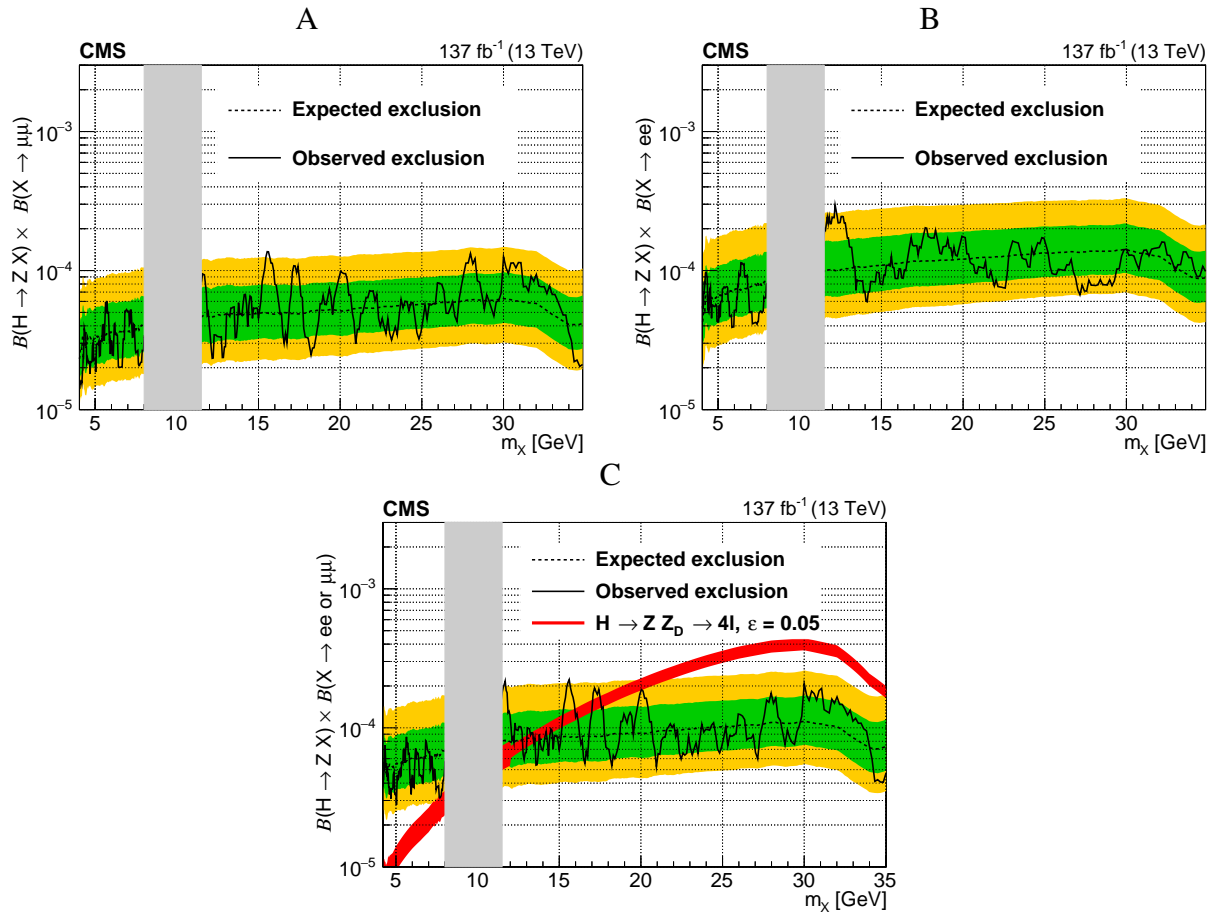
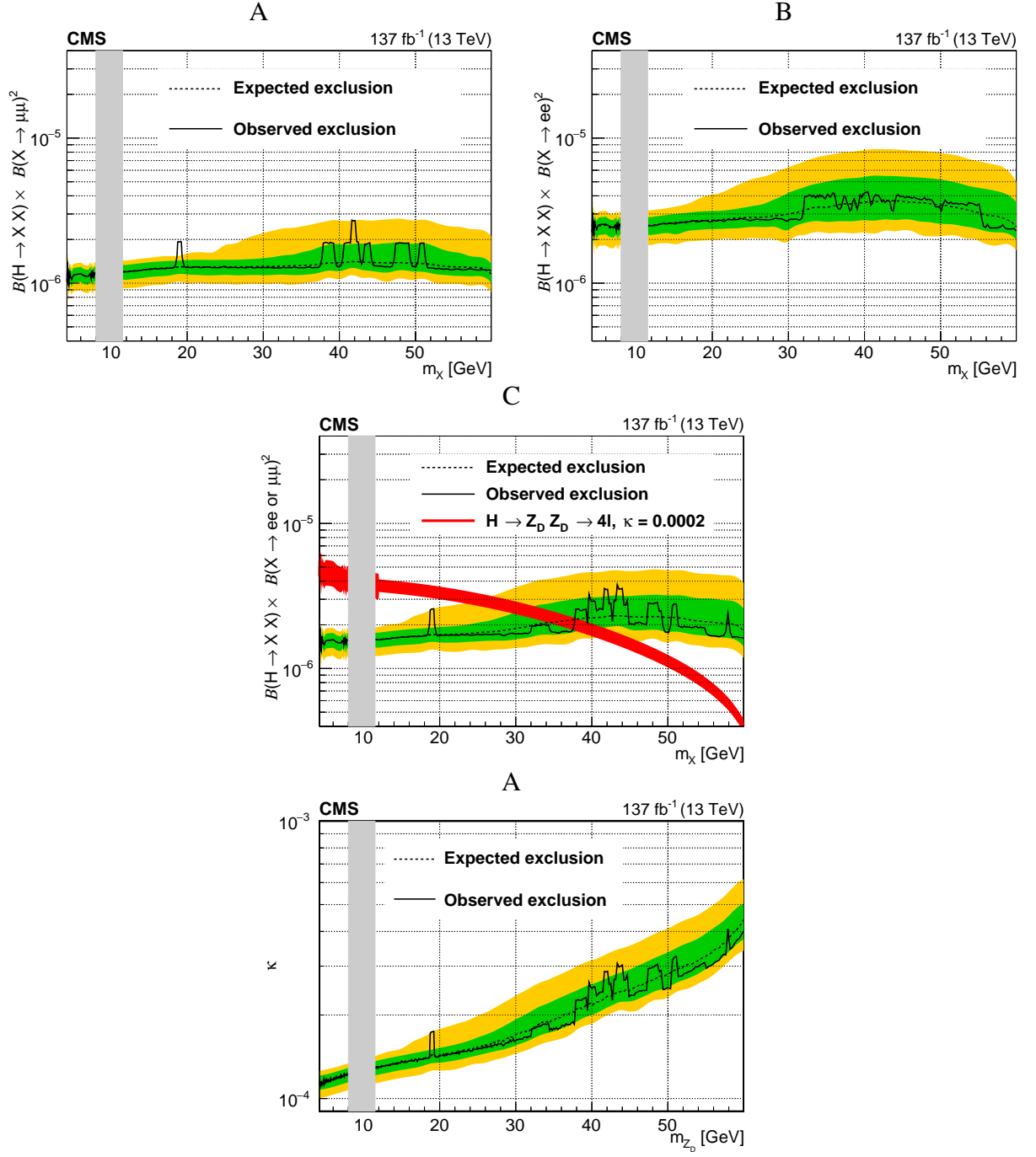


Figure 2-3



REFERENCES

- [1] PARTICLE DATA GROUP collaboration, *Review of particle physics*, *Progress of Theoretical and Experimental Physics* **2020** (2020) 083C01.
- [2] G. Cowan, K. Cranmer, E. Gross and O. Vitells, *Asymptotic formulae for likelihood-based tests of new physics*, *Eur. Phys. J. C* **71** (2011) 1554.

BIOGRAPHICAL SKETCH

Jake Rosenzweig had the best childhood anyone could ask for, growing up in Jacksonville, FL: enjoying video games with excellent friends, playing football on the beach, and having plenty of opportunity to make mistakes. He graduated from the University of Florida in 2011 with a B.S. in chemistry, while maintaining his sanity by getting minors in education and Latin. He enjoys building things from scrap, weightlifting, hiking in the Coloradoan mountains, gardening, silence, and—most of all—receiving the beleaguered stare from his wife after telling her a *particularly* bad dad joke.